Check for updates

Geophysical Research Letters

RESEARCH LETTER
10.1029/2020GL090348

Elucidating the Mechanisms Responsible for Hadley Cell Weakening Under 4 × CO_2 Forcing

R. Chemke[1,2] and **L. M. Polvani**[2,3]

[1]Department of Earth and Planetary Sciences, Weizmann Institute of Science, Rehovot, Israel, [2]Department of Applied Physics and Applied Mathematics, Columbia University, New York, NY, USA, [3]Department of Earth and Environmental Sciences and Lamont-Doherty Earth Observatory, Columbia University, Palisades, NY, USA

Key Points:

- Surface warming alone is unable to explain Hadley cell weakening under 4 × CO_2 forcing, as the weakening exhibits a much faster response
- Each of the previously proposed mechanisms analyzed in this study cannot fully explain the weakening of the Hadley cell
- The weakening stems from a combination of the opposing effects of increases in stratification and in meridional gradient of latent heating

Supporting Information:

- Supporting Information S1

Correspondence to:
R. Chemke,
rei.chemke@weizmann.ac.il

Citation:
Chemke, R., & Polvani, L. M. (2021). Elucidating the mechanisms responsible for Hadley cell weakening under 4 × CO_2 forcing. *Geophysical Research Letters*, *48*, e2020GL090348. https://doi.org/10.1029/2020GL090348

Received 13 AUG 2020
Accepted 13 DEC 2020

Abstract The projected weakening of the Northern Hemisphere Hadley cell will have large climatic impacts at low latitudes. Several mechanisms have been proposed to explain this weakening. In order to isolate and assess their relative importance, we here use the abrupt 4 × CO_2 experiment of the Coupled Model Intercomparison Project phase 5, as this forcing separates the different mechanisms which respond on different time scales. We find that the Hadley circulation responds relatively quickly to quadrupling CO_2 concentrations, reaching its steady-state value after less than a decade. This fast response demonstrates that the weakening could not be solely due to the much slower increase in surface temperature. In addition, we show that the Hadley cell's weakening results from a combination of an increase in tropical static stability, partially offset by an increase in the latitudinal gradient of latent heating.

Plain Language Summary The Hadley circulation has large effects on the variability of temperature and precipitation at low latitudes. By the end of the 21st century, climate models project a weakening of the circulation, which will have great societal impacts. It is thus critical to elucidate the underlying mechanisms of the projected weakening. Here, we assess different mechanisms for the projected weakening and show that it stems from an increase in the vertical temperature gradient in the tropics, which is partially offset by an increase in latent heating.

1. Introduction

Climate models project that the Hadley circulation (HC) will widen and weaken by the end of the 21st century (IPCC, 2013; Vallis et al., 2015). These circulation changes will have large societal impacts, affecting tropical and subtropical precipitation (IPCC, 2014). Note that changes in the HC are fundamentally different between the two hemispheres. The expansion of the circulation is projected to occur mostly in the Southern Hemisphere (SH) (Grise et al., 2019; Vallis et al., 2015). Over recent decades, reanalyses show a modest expansion of the SH HC (Davis & Davis, 2018; Grise et al., 2019), mostly driven by ozone depletion in the second half of the 20th century (Polvani et al., 2011; Son et al., 2009). With the unabated emissions of greenhouse gases into the atmosphere, the expansion in the SH is projected to emerge out of the internal variability by the mid-21st century (Grise et al., 2019). Over the last decades, several mechanisms have been proposed to explain the expansion of the HC (arguing that is caused by changes in sea surface temperature, eddy phase speed, tropopause height, static stability, etc.). Recently, by examining the HC response in the abrupt 4 × CO_2 experiment of the Coupled Model Intercomparison Project phase 5 (CMIP5), we showed that changes in static stability are the key factor in tropical expansion (Chemke & Polvani, 2019a), thus confirming previous studies who argued for its importance (Lu et al., 2008; Son et al., 2018; Vallis et al., 2015). It is also important to note that HC expansion in the Northern Hemisphere (NH) is not projected to emerge from the internal variability between now and the end of this century (Grise et al., 2019).

Unlike the expansion of the tropical circulation, its weakening is projected to occur only in the NH (Figures 1a and 1b). Interestingly, over the last several decades, while climate models simulate a weakening of the NH HC, reanalyses indicate an erroneous strengthening. This discrepancy was recently shown to be due to artifacts in the representation of latent heating in reanalyses (Chemke & Polvani, 2019b).

Several mechanisms have been proposed to explain the NH HC weakening. We start with a brief review of six mechanisms that we analyze in this study. The first two mechanisms constrain the vertical flow using

© 2020. American Geophysical Union. All Rights Reserved.

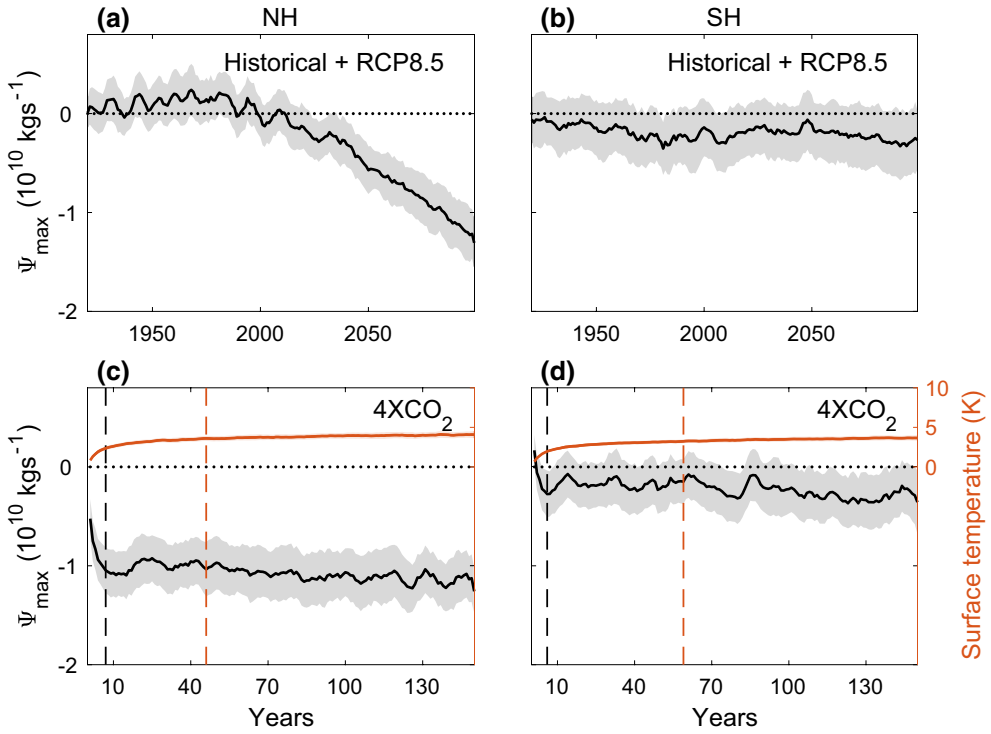

Figure 1. Time series, relative to PI, of NH (left column) and SH (right column) HC strength (Ψ_{max}, 10^{10}, kg s^{-1}) under the historical and RCP8.5 scenarios (upper row) and under the abrupt 4 × CO_2 experiment (bottom row). The orange lines show the time series of tropical mean surface temperature (K). The vertical dashed lines show the response time of each quantity. The shadings in all panels represent the 95% confidence interval calculated via Student's *t*-distribution across all models. PI, preindustrial; NH, Northern Hemisphere; SH, Southern Hemisphere; HC, Hadley circulation.

moisture or thermodynamic balances. The first, proposed by Held and Soden (2006), posits the balance $P = Mq$ between the convective flux (M) of boundary-layer mixing ratio (q) and precipitation (P). Under increased greenhouse gases, the faster increase in q with temperature (following the Clausius–Clapeyron relation) relative to P yields weaker convective fluxes. Since this balance mostly holds in the deep tropics, the suggested decline in M was found to correlate with the decline in tropical upward vertical velocity across the IPCC AR4 models (Vecchi & Soden, 2007). The second mechanism, based on the thermodynamic balance $\omega\theta_p = Q$, argues that the increase in diabatic heating (Q) with increased greenhouse gases is mostly balanced by changes in the vertical potential temperature gradient (θ_p), thus precluding intensification of the vertical velocity (ω) (Gastineau et al., 2008; Knutson & Manabe, 1995). Furthermore, should Q not increase as rapidly as θ_p, ω would decrease (Held & Soden, 2006).

The next two mechanisms argue that the direct radiative effects of CO_2 on the temperature act to weaken the circulation. The first was aimed at explaining the fast decline in tropical circulation strength in CMIP5 models under abrupt 4 × CO_2 concentrations (Bony et al., 2013): increasing CO_2 concentration acts to warm the atmosphere, by reducing the outgoing longwave radiation (OLR) more than the net surface heating, and this acts to stabilize the atmosphere, thus weakening the circulation. The second mechanism argues that the reduction in OLR (i.e., reduced heat loss), due to the increase in CO_2 concentrations, is smaller in the descending branch than in the ascending branch of the circulation (due to the different longwave absorption by clouds across the tropics), and this difference reduces the meridional heat transport from low to subtropical latitudes (Merlis, 2015).

The last two mechanisms focus on the importance of changes in the temperature gradients. The first argues that changes in stratification, advected by the vertical background flow, act to weaken the HC in the Northern Hemisphere (Ma et al., 2012), as was also suggested in Vallis et al. (2015). The second, proposed by Seo et al. (2014), is based on the Held and Hou (1980) scaling theory, and argues that the weakening of the NH

HC by the end of the 21st century is due to a reduction in the meridional temperature difference between the tropics and subtropical-to-midlatitudes, as was also suggested in Gastineau et al. (2009).

One reason for the existence of multiple mechanisms to explain a single physical phenomenon is the strong coupling among different components in the climate system. Such coupling results in high correlations between the changes in the circulation and several climate components: this makes it very difficult to assess the relative importance of these components in affecting the circulation. To overcome this, and elucidate which mechanism is mostly responsible for weakening the NH HC, we here employ the same methodology as in Chemke and Polvani (2019a), and analyze the abrupt $4 \times CO_2$ experiment of CMIP5. Such strong and abrupt forcing (quadrupling of CO_2 concentrations) separates the mechanisms operating on different time scales and, by studying their transient response, allows us to quantify which component contributes the most to the weakening of the NH HC. A caveat: while some of the mechanisms mentioned above were not originally developed to explain the projected weakening of the HC, but rather to explain the weakening of the Walker circulation (e.g., Knutson & Manabe, 1995) or tropical convection (e.g., Held & Soden, 2006), we nonetheless examine them here, since they are often claimed to explain the weakening of the HC (e.g., Lu et al., 2008; Vallis et al., 2015).

2. Methods

We analyze 20 CMIP5 models (listed in Table S1) under the "r1i1p1" realization in four experiments: pre-industrial (PI), historical and RCP8.5, and abrupt $4 \times CO_2$. The strength of the HC (Ψ_{max}) is defined by the maximum value at 500 mb of the meridional mass streamfunction (Ψ),

$$\Psi(\phi, p) = \frac{2\pi a \cos\phi}{g} \int_0^p \overline{v}(\phi, p) dp', \tag{1}$$

where ϕ is latitude, p is pressure, a is Earth's radius, g is gravity, v is meridional velocity, and overbar represents zonal and annual mean. To properly examine the proposed mechanisms across all models, the different regions and quantities for each mechanism are defined as follows:

1. The ascending branch of the HC is defined between the Inter Tropical Convergence Zone (ITCZ, where Ψ changes sign at 500 mb between the SH and NH HCs) and the latitude of Ψ_{max}. Given the different responses of the HC between the hemispheres, we do not define the ascending branch over the other side of the ITCZ, in order to avoid including processes that are not relevant for the weakening of the NH HC.
2. The descending branch of the HC is defined between the latitude of Ψ_{max} and the edge of the HC. The latter is defined as the latitude where Ψ first changes sign northward of the latitude of Ψ_{max} after a 0.1° latitudinal cubic interpolation.
3. To evaluate the Held and Soden (2006) mechanism, we calculate Pq^{-1} by averaging the precipitation and, following Held and Soden (2006), the column-integrated specific humidity over the ascending branch of the circulation. Using the saturated specific humidity, or the vertical specific humidity gradient (Schneider et al., 2010), yields similar results.
4. We follow Knutson and Manabe (1995) and calculate $\mathrm{OLR}\,\theta_p^{-1}$ over the descending branch, where θ_p is vertically integrated throughout the tropical troposphere (between 200 and 850 mb). We evaluate the mechanism over the descending branch only, since over the ascending branch their mechanism also includes latent heating, which is not available in the above CMIP5 models.
5. The mechanism by Bony et al. (2013) is evaluated by taking the difference between the OLR and net longwave radiative surface heating over the ascending branch ($\mathrm{OLR} - Q_{srf}$).
6. To analyze the mechanism by Merlis (2015), we calculate the difference in OLR between the descending and ascending branches (OLR_y).
7. To examine the role of static stability (Ma et al., 2012), we average the tropical tropospheric θ_p over the ascending branch.
8. Following Seo et al. (2014) we estimate the meridional potential temperature difference between the tropics and higher latitudes (θ_y) as the tropospheric (averaged between the surface and 400 mb) difference between the ascending branch and extratropics (averaged between the edge of the HC and 50°N).

To quantitatively compare the time evolution of each quantity with the time evolution of the HC strength, for any quantity $\chi(t)$ we plot its fractional change $\Delta\chi(t)$,

$$\Delta\chi(t) = 100\frac{\chi(t) - \chi_{\mathrm{PI}}}{\left|\chi_{\mathrm{PI}}\right|}, \tag{2}$$

where χ_{PI} denotes the value of the last 200 years from the PI. Finally, we calculate the response time of each quantity, defined by the first year a quantity reaches 90% of its steady-state value (the last 50 years of simulation). Choosing a different percentage cut-off value do not qualitatively changes the results.

3. Comparing the Two Hemispheres

Before examining the fractional changes in the HC under the abrupt $4 \times CO_2$ forcing, we first show (in absolute values) in Figure 1 that the projected weakening of the HC occurs mostly in the NH. By the end of the 21st century the multimodel mean NH Ψ_{max} is 16% weaker (it reduced by 1.2×10^{10} kg s^{-1}) than the PI value under the RCP8.5 scenario (Figure 1a). In contrast, the SH Ψ_{max} is only 3% smaller (Figure 1b). Thus, for the remainder of this manuscript, we will focus on the weakening of NH Ψ_{max}.

The different response of the HC in both hemispheres is also apparent in the abrupt $4 \times CO_2$ experiment: the NH Ψ_{max} reduces by 14%, while the SH Ψ_{max} by only 3% (black lines in Figures 1c and 1d). The similar response of Ψ_{max} to quadrupling CO_2 concentrations and to the RCP8.5 forcing provides us the confidence to elucidate the mechanism of HC weakening under the abrupt $4 \times CO_2$ experiment.

Before analyzing the different mechanisms, it is important to assess whether the response of Ψ_{max} to increased CO_2 concentrations is merely a response to the increase in surface temperature. The solid orange line in Figure 1c shows the time evolution of NH tropical surface temperature. Similar to other dynamic quantities (Chemke & Polvani, 2019a; Grise & Polvani, 2017), Ψ_{max} also shows a fast response to quadrupling CO_2 concentrations: it weakens in the first years of the simulation, with a response time of 7 years (black dashed vertical line in Figure 1c). In comparison, the tropical mean surface temperature shows a slower response time of 47 years (orange dashed vertical line), which demonstrates that the weakening of the circulation is not only due to the (slower) increase in surface temperature: one degree of surface warming in the early years might have a larger effect on Ψ_{max} than one degree of surface warming later in the simulation (Figure S1).

4. Evaluating the Mechanisms

Since some of the mechanisms discussed here were studied using either a single model or the previous generation of models (CMIP3), we first evaluate the robustness of each mechanism in the CMIP5 models. This is done by plotting the steady-state (the last 50 years of the $4 \times CO_2$ experiment) fractional change (relative to PI, denoted by Δ, see Equation 2) in Ψ_{max} against the change in key quantities relevant to each of the six mechanisms reviewed in Section 1 (Figure 2, left and middle columns).

We start with the mechanisms that constrain the vertical flow using moisture or thermodynamic balances. The changes in the Held and Soden (2006) estimate for the tropical mass flux (Pq^{-1}) shows a moderate correlation ($r = 0.56$) with the weakening of Ψ_{max} across the models (Figure 2a). However, Pq^{-1} overestimates the weakening of Ψ_{max} by ~50%. This overestimate led Held and Soden (2006) to note that changes in mass flux are clearly insufficient to explain the weakening of the Hadley cell. Changes in $\mathrm{OLR}\,\theta_p^{-1}$ (Gastineau et al., 2008; Knutson & Manabe, 1995) also show a moderate correlation ($r = 0.57$) with the weakening of Ψ_{max} across the models (Figure 2b). Note, however, that $\mathrm{OLR}\,\theta_p^{-1}$ slightly underestimates the weakening of Ψ_{max}. Thus, unlike previous claims (e.g., Held & Soden, 2006), these two mechanisms might not be equivalent.

Next, we evaluate the mechanisms that argue for the importance of the direct radiative effects of CO_2 on temperature, by plotting the first-year fractional change (denoted by δ) in Ψ_{max} against the quantities of each mechanism. We focus on the first year, rather on the steady state, since these mechanisms aim to explain the direct fast response of the circulation to quadrupling CO_2 concentrations without the slow warming of

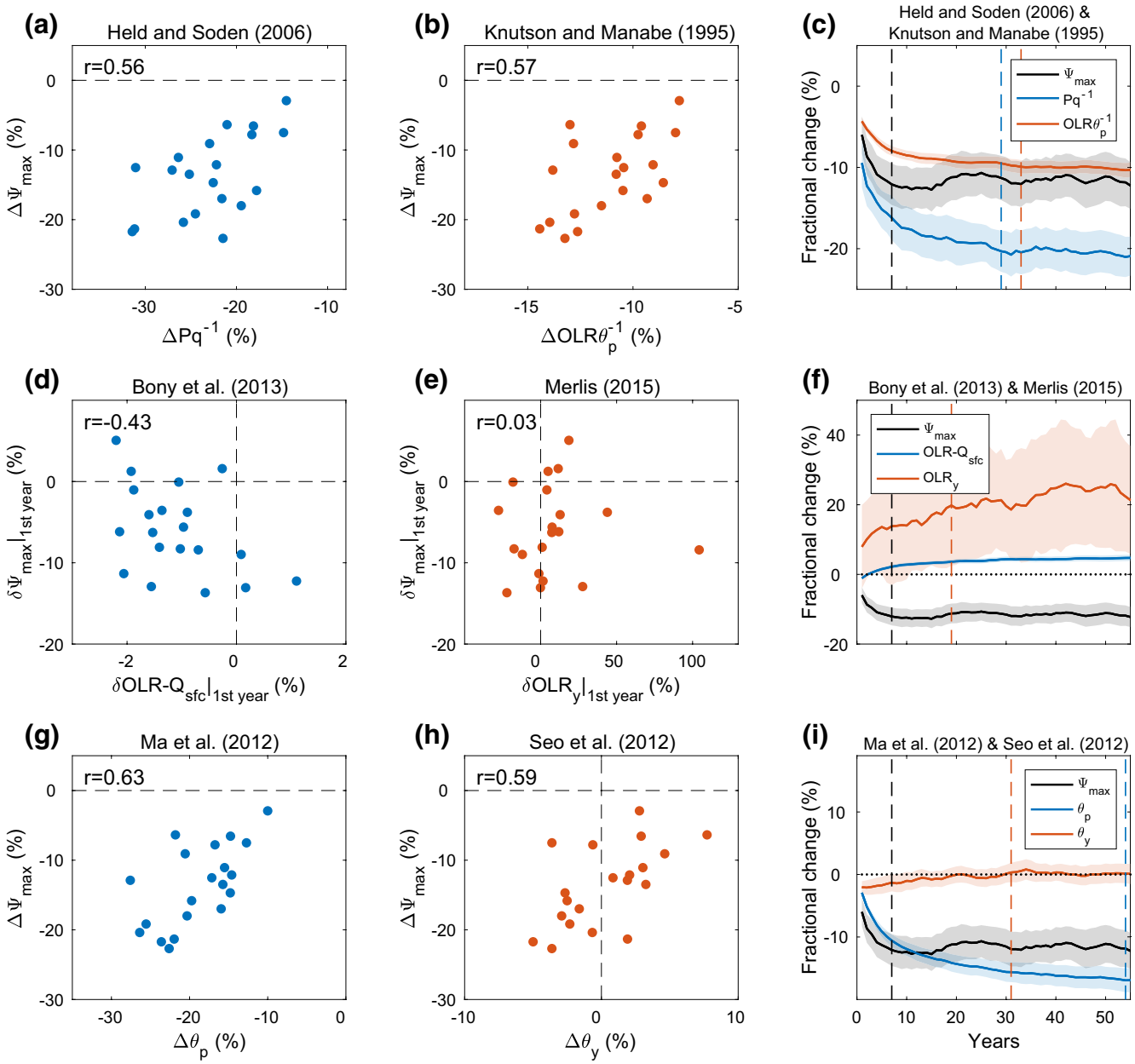

Figure 2. The fractional change (in %, relative to PI) in NH Ψ_{max} under the abrupt 4 × CO_2 forcing vs. the fractional change in each of the mechanisms, as indicated by the quantities: (a) Pq^{-1}, (b) $\mathrm{OLR}\theta_p^{-1}$, (d) OLR − Q_{srf}, (e) OLR_y, (g) θ_p, and (h) θ_y. Panels a, b, g, and h show the steady-state changes, while panels c and d show the first year changes. Time series of the fractional change (in %, relative to PI) under the abrupt 4 × CO_2 forcing in NH Ψ_{max} (black lines) and in each of the mechanisms as indicated by the quantities: (c) Pq^{-1} (blue line) and $\mathrm{OLR}\theta_p^{-1}$ (red line), (f) OLR − Q_{srf} (blue line) and OLR_y (red line), and (i) θ_p (blue line) and θ_y (red line). The vertical dashed lines show the response time of each quantity. The shadings represent the 95% confidence interval calculated via Student's *t*-distribution across all models. PI, preindustrial; NH, Northern Hemisphere; OLR, outgoing longwave radiation.

the surface. Although, as suggested by Bony et al. (2013), most models (17 out of 20) indeed show that in year-1 the OLR reduces faster than the net surface heating (OLR − Q_{srf}, negative *x* axis values in Figure 2d), it has a low correlation ($r = -0.43$) with the weakening of Ψ_{max} across the models, thus unlikely to explain the fast response of Ψ_{max}.

Not only the effects of CO_2 on the vertical temperature profile show low correlation with the weakening of Ψ_{max}, but also the CO_2 effects on the meridional temperature structure (Figure 2e). The first-year fractional change in OLR_y (Merlis, 2015) also shows low correlation ($r = 0.03$, and $r = 0.19$ excluding the rightmost

outlier point) with the weakening of Ψ_{max} across the models. Furthermore, unlike the single model used in Merlis (2015), most CMIP5 models analyzed here (13 out of 20) show that the OLR reduces more over the ascending branch than the descending branch (positive x axis values), which, according to Merlis (2015) argument, would result in a strengthening of the HC. Clearly, changes in OLR_y cannot explain the weakening of Ψ_{max}.

Lastly, we evaluate the mechanisms that argue for the importance of changes in the temperature gradients. Both steady-state fractional changes in θ_p (Ma et al., 2012) and θ_y (Seo et al., 2014) (see Figures 2g and 2h, respectively) show moderate correlations with the weakening of Ψ_{max} across the models: correlation of $r = 0.63$ for θ_p and of $r = 0.59$ for θ_y. In agreement with the weakening of Ψ_{max} across all models, θ_p also shows a decline under $4 \times CO_2$ (corresponding to a more stable atmosphere) in all models. On the other hand, only half of the models show a decline in θ_y at steady state, while the other half show an increase. This major disagreement across the CMIP5 models suggests that θ_y cannot explain the steady-state weakening of Ψ_{max} across all models.

As mentioned in Section 1, one reason for the existence of correlations between multiple metrics and the weakening of Ψ_{max} is the strong coupling between the different components of the climate system. Note that while most quantities do not correlate with each other, the quantities that do show a moderate correlation with Ψ_{max} (Pq^{-1}, $\mathrm{OLR}\theta_p^{-1}$ and θ_p) also correlate with each other (Held & Soden, 2006) (Table S2). In particular, $\mathrm{OLR}\theta_p^{-1}$ and θ_p are highly correlated, with $r = 0.92$, suggesting that these two mechanisms are not entirely distinct. Next, to further examine how the above quantities are related to Ψ_{max}, and to disentangle them, we investigate their time evolution (blue and red lines in right column in Figure 2), and compare it to the evolution of Ψ_{max} (black lines in right column in Figure 2). Since most of the weakening of Ψ_{max} occurs in the first years, we zoom in on the evolution over the first 55 years.

Starting from Pq^{-1} (Held & Soden, 2006), one can see in Figure 2c that it severely overestimates the weakening of Ψ_{max} throughout the entire period (compare blue and black lines). Most importantly, in spite of the steady-state correlation across models between Pq^{-1} and Ψ_{max} (Figure 2a), the evolution of Pq^{-1} clearly does not accompany the evolution of Ψ_{max}: it does not capture the strong weakening of Ψ_{max} in the first few years, resulting in a slower response time of 29 years (blue dashed vertical line), compared to the fast 7-years response time of Ψ_{max} (black dashed vertical line). This mismatch between Ψ_{max} and Pq^{-1} confirms previous studies (e.g., Chou & Chen, 2010; Held & Soden, 2006; Schneider et al., 2010) who also argued that the Held and Soden (2006) balance is insufficient for explaining the weakening of the HC. Similarly, in spite of the steady-state correlation between $\mathrm{OLR}\theta_p^{-1}$ and Ψ_{max} (Figure 2b) the evolution of $\mathrm{OLR}\theta_p^{-1}$ (Gastineau et al., 2008; Knutson & Manabe, 1995) does not coincide with the evolution of Ψ_{max} (compare red and black lines in Figure 2c): it does not capture the fast response in the first years, and it has a considerably slower response time of 33 years (red dashed vertical line). Furthermore, $\mathrm{OLR}\theta_p^{-1}$ underestimates the weakening of Ψ_{max}, not only at steady state, but also throughout the entire simulation.

Next we examine, in Figure 2f, the evolution of the radiative effects of CO_2 on temperature. First, as argued in Bony et al. (2013), the response of $\mathrm{OLR} - Q_{srf}$ should explain the fast weakening of Ψ_{max} before the increase in surface temperature. Indeed, $\mathrm{OLR} - Q_{srf}$ decreases only in the first two years (blue line in Figure 2f, see the initially small negative values in $\mathrm{OLR} - Q_{srf}$), and then increases as the surface warms. However, the low correlation between $\mathrm{OLR} - Q_{srf}$ and Ψ_{max} even in the first years suggests that this mechanism does not explain the fast weakening of Ψ_{max}. Second, not only does the mechanism proposed by Merlis (2015) not hold at the first years (Figure 2e), but also throughout the entire time evolution (red line in Figure 2f): if that mechanism were operative, a strengthening, not a weakening, of the HC occur, since the OLR decreases more over the ascending than over the descending branch (see how $\mathrm{OLR} - Q_{srf}$ is positive for the entire simulation).

Finally, we examine the time evolution of temperature gradients. Although θ_p decreases in all models and correlates with Ψ_{max} (Figure 2g) its evolution does not coincide with the evolution of Ψ_{max} (blue line in Figure 2i): it shows a much slower response (of 54 years, blue dashed vertical line). Similarly, in spite of the correlation between θ_y and Ψ_{max} at steady state (Figure 2h), the evolution of θ_y is very different than the evolution of Ψ_{max} (red line in Figure 2i). In the first year, θ_y indeed shows a decline relative to PI, in accordance with the argument by Seo et al. (2014); however, it then increases, while at the same time Ψ_{max} monotonically weakens. This again suggests that θ_y is not likely to explain the weakening of Ψ_{max}.

5. The Kuo-Eliassen Equation

Having shown that none of the above mechanisms is able to solely explain the weakening of the HC, we build on our previous work (Chemke & Polvani, 2018, 2019b; Chemke et al., 2019; Vallis et al., 2015), and investigate the Kuo-Eliassen (KE) equation, in order to isolate and quantify the terms that affect the HC response. The KE equation is derived from quasigeostrophic arguments (cf. Section 14.5.5 in Peixoto and Oort (1992)) and takes the following form:

$$L\Psi = D_Q + D_{\overline{v'T'}} + D_{\overline{u'v'}} + D_X, \tag{3}$$

where $L = f^2 \frac{g}{2\pi a \cos\phi}\frac{\partial^2}{\partial p^2} + S^2 \frac{g}{2\pi a}\frac{\partial}{a\partial\phi}\frac{1}{a\cos\phi}\frac{\partial}{\partial\phi}$ is a second-order elliptic operator, f is the Coriolis parameter, $S^2 = -\frac{1}{\rho\theta}\frac{\partial\theta}{\partial p}$ is static stability, ρ is density, $D_Q = \frac{R}{p}\left(\frac{1}{a}\frac{\partial\overline{Q}}{\partial\phi}\right)$, R is the gas constant of dry air, Q is diabatic heating, $D_{\overline{v'T'}} = -\frac{R}{p}\left(\frac{\partial}{a\partial\phi}\frac{1}{a\cos\phi}\frac{\partial\overline{v'T'}\cos\phi}{\partial\phi}\right)$, $\overline{v'T'}$ is eddy heat flux, $D_{\overline{u'v'}} = f\left(\frac{1}{a\cos^2\phi}\frac{\partial^2\overline{u'v'}\cos^2\phi}{\partial p\partial\phi}\right)$, $\overline{u'v'}$ is eddy momentum flux and $D_X = -f\frac{\partial\overline{X}}{\partial p}$, where X is zonal friction; bars and primes represent zonal and monthly means, and deviation therefrom, respectively.

Using a successive overrelaxation method, we numerically solve Equation 3 with the right-hand side terms, and S^2 from the left-hand side operator, calculated from four models (GFDL-ESM2G, GFDL-ESM2M, MIROC5, and IPSL-CM5B-LR). We use these four models because they are the only ones for which daily output for calculating eddy fluxes and diabatic heating is available. We use the thermodynamic equation, $Q = \frac{DT}{Dt} - \frac{\omega TR}{pc_p}$, to estimate the diabatic heating, where $\frac{D}{Dt} = \frac{\partial}{\partial t} + \mathbf{V}\cdot\nabla$, $\mathbf{V} = (u, v, \omega)$, and c_p is specific heat capacity, and the mean zonal momentum quasigeostrophic equation, $\overline{X} = \frac{1}{a\cos^2\phi}\frac{\partial^2\overline{u'v'}\cos^2\phi}{\partial\phi^2} - f\overline{v}$, to estimate the zonal friction. As for Ψ_{max}, the maximum value of the solution for Equation 3 (Ψ^{KE}_{max}) is evaluated at 500 mb.

Since the KE equation is derived under quasigeostrophic assumptions, which do not hold in the deep tropics, it needs not, a priori, capture the response of Ψ_{max} to increased greenhouse gases. However, the KE equation comprises key processes that control Ψ_{max} (e.g., diabatic heating, static stability, eddy fluxes). Furthermore, note that unlike in quasigeostrophic theory, here both f^2 and S^2 vary in space, in order to examine the effect of changes of S^2 on Ψ_{max}, and to allow the KE equation to better capture the circulation of low latitudes. Thus, as shown below, the KE equation well captures the behavior of Ψ_{max}.

First, we demonstrate that the evolution of Ψ^{KE}_{max} is very close to the evolution of Ψ_{max} (compare black and blue lines in Figure 3a): it not only captures the strong weakening in the first years, but also the interannual variability throughout the entire simulation (this occurs in each of the four models, Figure S2). As a result, the time response of Ψ^{KE}_{max} (10 years, blue vertical dashed line) is close to the time response of Ψ_{max} (black vertical dashed line). The good agreement between Ψ^{KE}_{max} and Ψ_{max}, together with the fact that Equation 3 is linear, allow us to determine which RHS terms most contribute to the weakening of the circulation, and to evaluate the signature of static stability in the L operator on the LHS (e.g., Chemke & Polvani, 2019b).

We follow Kim and Lee (2001), and decomposed each of the terms in Equation 3 into their PI value and a change from it: $L = L_{PI} + \delta L$, $\Psi = \Psi_{PI} + \delta\Psi$ and $D = D_{PI} + \delta D$. Substituting these decompositions to Equation 3 yields an equation for the changes in Ψ ($\delta\Psi$),

$$L_{PI}\delta\Psi = \delta D - \delta L\Psi_{PI} - \delta L\delta\Psi, \tag{4}$$

where δD accounts for changes in each of the RHS terms in Equation 3, $\delta L\Psi_{PI}$ accounts for changes in the static stability, and $\delta L\delta\Psi$ accounts for the multiplicative changes in static stability and in the streamfunction (calculated as a residual).

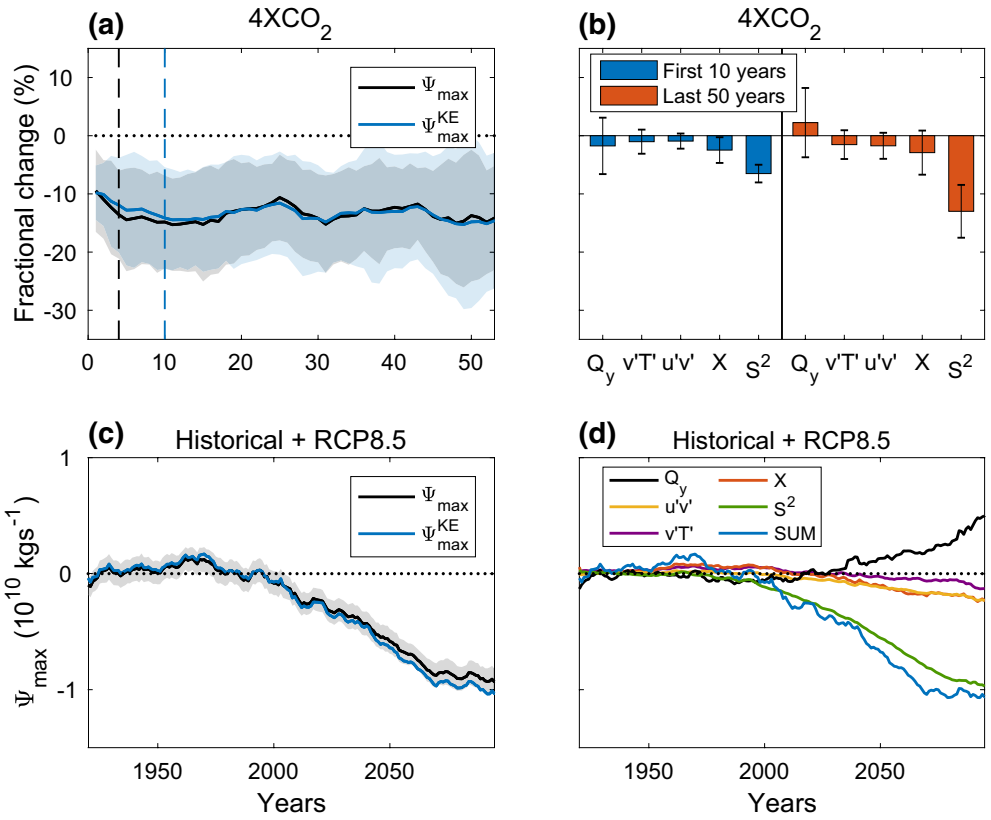

Figure 3. Time series, relative to PI, of NH Ψ_{max} (black line), and Ψ^{KE}_{max} (blue line) of (a) their fractional change (in %) under the abrupt $4 \times CO_2$ forcing in CMIP5, and (c) their absolute values (10^{10}, kg s^{-1}) under the historical and RCP8.5 forcing in CESM LE. The vertical dashed lines show the response time of each quantity. The relative contributions to changes in Ψ^{KE}_{max} under (b) the abrupt $4 \times CO_2$ forcing in CMIP5, and (d) historical and RCP8.5 forcing in CESM LE from: diabatic heating (Q_y), eddy heat fluxes ($v'T'$), eddy momentum fluxes ($u'v'$), zonal friction (X) and static stability (S^2). In panel b blue and red bars show the relative contributions to the first 10 years and last 50 years fractional change in Ψ^{KE}_{max}, respectively. Blue line in panel d shows the sum from all contributions. The shadings and error bars represent the 95% confidence interval calculated via Student's t-distribution across all simulations. PI, preindustrial; NH, Northern Hemisphere; LE, large ensemble; CESM, Community Earth System Model; CMIP5, Coupled Model Intercomparison Project phase 5.

Figure 3b shows the contributions from each term in Equation 3 to changes in Ψ^{KE}_{max} (i.e., the terms are estimated at the location of Ψ^{KE}_{max}) over the first 10 years (the fast response, blue bars), and over the last 50 years (steady-state response, red bars). As suggested by Ma et al. (2012) and Vallis et al. (2015), the term that mostly contributes to the weakening of Ψ^{KE}_{max} in both periods is static stability (S^2). Since static stability exhibits a slower response than Ψ_{max} (Figure 2i), it cannot solely explain the fast response of Ψ_{max}. Another component needs to oppose the slow increase in static stability (recall that $S^2 \sim -\partial\theta/\partial p$, and thus increases in all models), and yield in the faster response of Ψ_{max}. Interestingly, it is the meridional gradient of diabatic heating (Q_y), not the diabatic heating itself (as was previously suggested, Gastineau et al., 2008; Knutson & Manabe, 1995), that acts to weaken the circulation in the initial stages, but to strengthen it at steady state. This Q_y opposes the slow increase in static stability, and results in the fast 7-years response time of Ψ_{max}. The other components (e.g., eddy fluxes) have minor contributions to the weakening the HC, and show little change with time, and thus could not oppose the contribution of S^2 (these results are robust across all four models, Figure S2). Note that Q_y shows the largest spread across the models, suggesting that it might be responsible for the large spread in the projected weakening of the HC across CMIP5 models (Chemke & Polvani, 2019b).

To corroborate the importance of S^2 and Q_y (and their opposite effects on the circulation), and to verify that the $4 \times CO_2$ results hold in a more realistic scenario, and with many more models (which increases the

significance of the result), we repeat the above analysis under the historical and RCP8.5 forcing using the CESM large ensemble (LE). The LE comprises 40 simulations that are subjected to the historical and RCP8.5 forcing between 1920 and 2100 (Kay et al., 2015). Figure 3c shows the evolution of Ψ_{max} from the LE (black), along with the solution from Equation 3 (blue). First, through most of the simulation, the evolution of Ψ_{max} from the LE is similar to the evolution of the CMIP5 models in Figure 1a. This gives us confidence to use the LE to understand the weakening of the HC. Second, as for the abrupt $4 \times CO_2$ experiment, here too the evolution of Ψ^{KE}_{max} is very close to the evolution of Ψ_{max}.

Armed with these validations, we now decompose the evolution of Ψ^{KE}_{max} into the different components (see Equation 3), and plot these in Figure 3d. First, the sum of all components (except for a small residual) is very similar to Ψ^{KE}_{max} (compare blue lines in Figures 3c and 3d): this allows us to quantify their relative importance. Second, the key results obtained from the abrupt $4 \times CO_2$ experiment also hold under the historical and RCP8.5 forcing: the HC weakens as a consequence of S^2 (green line), with important cancelation from changes in Q_y (black line). Most of the effect of Q_y originates from the meridional gradient of latent heating ($Q_y|_{latent}$, Figure S3). Thus, the increase in latent heat release at upper levels over the ascending branch results in two opposite effects on the tropical circulation. On the one hand, it acts to increase $Q_y|_{latent}$, and to strengthen the circulation. On the other hand, it acts to stabilize the atmosphere, which overcomes the effect of $Q_y|_{latent}$, and eventually to weaken the circulation. The other components play only a minor role in weakening the HC. Finally, we note that the different components in Equation 3 are not independent. Thus, the contribution of Q_y and S^2 may stem from changes in the other terms (as noted in Kim and Lee (2001)).

6. Conclusions

Analyzing the output of 20 CMIP5 models forced with $4 \times CO_2$, we have been able to shed new light on the mechanism underlying the ongoing and projected weakening of the HC, as that abrupt forcing effectively separates physical responses occurring on different time scales. First we have shown that, as for HC expansion (Chemke & Polvani, 2019a; Grise & Polvani, 2017), HC weakening occurs on much faster time scales than surface temperature warming, and is thus not a simple response to the increases in surface temperature alone. Second, we have revisited and evaluated six well-known mechanisms proposed to explain HC weakening (Bony et al., 2013; Held & Soden, 2006; Knutson & Manabe, 1995; Ma et al., 2012; Merlis, 2015; Seo et al., 2014). While some correlation across the models is suggestive of some of these mechanisms playing a potential role, we have shown that each mechanism alone cannot fully explain the weakening of the HC as they all fail to capture its time evolution under $4 \times CO_2$ forcing. Instead, we have explicitly shown that HC weakening results from an increase in static stability (as was previously suggested, Ma et al., 2012; Vallis et al., 2015), but with a considerable cancelation by an increase in the meridional gradient of latent heating.

Acknowledgments
We would like to thank Geoff Vallis and another anonymous reviewer for their very useful comments. R. Chemke and L. M. Polvani are founded by grants from the National Science Foundation to Columbia University. The CMIP5 data are available at https://esgf-node.llnl.gov/projects/cmip5/ and the CESM LE at http://www.cesm.ucar.edu/.

References

Bony, S., Bellon, G., Klocke, D., Sherwood, S., Fermepin, S., & Denvil, S. (2013). Robust direct effect of carbon dioxide on tropical circulation and regional precipitation. *Nature Geoscience*, *6*, 447–451.

Chemke, R., & Polvani, L. M. (2018). Ocean circulation reduces the Hadley cell response to increased greenhouse gases. *Geophysical Research Letters*, *45*, 9197–9205. https://doi.org/10.1029/2018GL079070

Chemke, R., & Polvani, L. M. (2019). Exploiting the abrupt 4xCO_2 scenario to elucidate tropical expansion mechanisms. *Journal of Climate*, *32*(3), 859–875.

Chemke, R., & Polvani, L. M. (2019). Opposite tropical circulation trends in climate models and in reanalyses. *Nature Geoscience*, *12*, 528–532.

Chemke, R., Polvani, L. M., & Deser, C. (2019). The effect of Arctic Sea ice loss on the Hadley circulation. *Geophysical Research Letters*, *46*, 963–972. https://doi.org/10.1029/2018GL081110

Chou, C., & Chen, C.-A. (2010). Depth of convection and the weakening of tropical circulation in global warming. *Journal of Climate*, *23*, 3019–3030.

Davis, N. A., & Davis, S. M. (2018). Reconciling Hadley cell expansion trend estimates in reanalyses. *Geophysical Research Letters*, *45*(20), 11439–11446. https://doi.org/10.1029/2018GL079593

Gastineau, G., Le Treut, H., & Li, L. (2008). Hadley circulation changes under global warming conditions indicated by coupled climate models. *Tellus A*, *60*, 863–884.

Gastineau, G., Li, L., & Le Treut, H. (2009). The Hadley and Walker circulation changes in global warming conditions described by idealized atmospheric simulations. *Journal of Climate*, *22*, 3993–4013.

Grise, K. M., Davis, S. M., Simpson, I. R., Waugh, D. W., Fu, Q., Allen, R. J., & Staten, P. W. (2019). Recent tropical expansion: Natural variability or forced response? *Journal of Climate*, *32*, 1551–1571.

Grise, K. M., & Polvani, L. M. (2017). Understanding the time scales of the tropospheric circulation response to abrupt CO_2 forcing in the Southern Hemisphere: Seasonality and the role of the stratosphere. *Journal of Climate*, *30*, 8497–8515.

Held, I. M., & Hou, A. Y. (1980). Nonlinear axially symmetric circulations in a nearly inviscid atmosphere. *Journal of the Atmospheric Sciences*, *37*, 515–533.

Held, I. M., & Soden, B. J. (2006). Robust responses of the hydrological cycle to global warming. *Journal of Climate*, *19*, 5686–5699.

IPCC. (2013). Climate change 2013: The physical science basis. In T. F. Stocker, D. Qin, G.-K. Plattner, M. Tignor, S. K. Allen, J. Boschung, et al. (Eds.), *Contribution of working group I to the fifth assessment report of the intergovernmental panel on climate change* (pp. 1585). Cambridge, UK: Cambridge University Press.

IPCC. (2014). Summary for policymakers. In C. B. Field, V. R. Barros, D. J. Dokken, K. J. Mach, M. D. Mastrandrea, T. E. Bilir, M. Chatterjee, et al. (Eds.), *Climate change 2014: Impacts, adaptation, and vulnerability*. Cambridge, UK: Cambridge University Press

Kay, J. E., Deser, C., Phillips, A., Mai, A., Hannay, C., Strand, G., & Vertenstein, M. (2015). The Community Earth System Model (CESM) large ensemble project: A community resource for studying climate change in the presence of internal climate variability. *Bulletin of the American Meteorological Society*, *96*, 1333–1349.

Kim, H.-K., & Lee, S. (2001). Hadley cell dynamics in a primitive equation model. Part I: Axisymmetric flow. *Journal of the Atmospheric Sciences*, *58*(19), 2845–2858.

Knutson, T. R., & Manabe, S. (1995). Time-mean response over the tropical Pacific to increased CO_2 in a coupled ocean-atmosphere model. *Journal of Climate*, *8*, 2181–2199.

Lu, J., Chen, G., & Frierson, D. M. W. (2008). Response of the zonal mean atmospheric circulation to El Niño versus global warming. *Journal of Climate*, *21*, 5835.

Ma, J., Xie, S.-P., & Kosaka, Y. (2012). Mechanisms for tropical tropospheric circulation change in response to global warming. *Journal of Climate*, *25*, 2979–2994.

Merlis, T. M. (2015). Direct weakening of tropical circulations from masked co2 radiative forcing. *Proceedings of the National Academy of Sciences of the United States of America*, *112*(43), 13167–13171.

Peixoto, J. P., & Oort, A. H. (1992). Physics of climate. College Park, MD: *American Institute of Physics*.

Polvani, L. M., Waugh, D. W., Correa, G. J. P., & Son, S. W. (2011). Stratospheric ozone depletion: The main driver of twentieth-century atmospheric circulation changes in the Southern Hemisphere. *Journal of Climate*, *24*, 795–812.

Schneider, T., O'Gorman, P. A., & Levine, X. J. (2010). Water vapor and the dynamics of climate change. *Reviews of Geophysics*, *48*, RG3001. 10.1029/2009RG000302

Seo, K.-H., Frierson, D. M. W., & Son, J.-H. (2014). A mechanism for future changes in Hadley circulation strength in CMIP5 climate change simulations. *Geophysical Research Letters*, *41*, 5251–5258. 10.1002/2014GL060868

Son, S.-W., Kim, S. Y., & Min, S. K. (2018). Widening of the Hadley cell from last glacial maximum to future climate. *Journal of Climate*, *31*, 267–281.

Son, S.-W., Tandon, N. F., Polvani, L. M., & Waugh, D. W. (2009). Ozone hole and Southern Hemisphere climate change. *Geophysical Research Letters*, *36*, L15705. 10.1029/2009GL038671

Vallis, G. K., Zurita-Gotor, P., Cairns, C., & Kidston, J. (2015). Response of the large-scale structure of the atmosphere to global warming. *Quarterly Journal of the Royal Meteorological Society*, *141*, 1479–1501.

Vecchi, G. A., & Soden, B. J. (2007). Global warming and the weakening of the tropical circulation. *Journal of Climate*, *20*, 4316–4340.